Interspecies activation correlations reveal functional correspondences between marmoset and human brain areas

Yuki Hori[a,1], Justine C. Cléry[a], Janahan Selvanayagam[b], David J. Schaeffer[c], Kevin D. Johnston[b], Ravi S. Menon[a], and Stefan Everling[a,b,1]

[a]Centre for Functional and Metabolic Mapping, Robarts Research Institute, The University of Western Ontario, London, ON N6A 5B7, Canada; [b]Department of Physiology and Pharmacology, The University of Western Ontario, London, ON N6A 5C1, Canada; and [c]Department of Neurobiology, University of Pittsburgh, Pittsburgh, PA 15213

Edited by Doris Y. Tsao, California Institute of Technology, Pasadena, CA, and approved August 9, 2021 (received for review June 14, 2021)

The common marmoset has enormous promise as a nonhuman primate model of human brain functions. While resting-state functional MRI (fMRI) has provided evidence for a similar organization of marmoset and human cortices, the technique cannot be used to map the functional correspondences of brain regions between species. This limitation can be overcome by movie-driven fMRI (md-fMRI), which has become a popular tool for noninvasively mapping the neural patterns generated by rich and naturalistic stimulation. Here, we used md-fMRI in marmosets and humans to identify whole-brain functional correspondences between the two primate species. In particular, we describe functional correlates for the well-known human face, body, and scene patches in marmosets. We find that these networks have a similar organization in both species, suggesting a largely conserved organization of higher-order visual areas between New World marmoset monkeys and humans. However, while face patches in humans and marmosets were activated by marmoset faces, only human face patches responded to the faces of other animals. Together, the results demonstrate that higher-order visual processing might be a conserved feature between humans and New World marmoset monkeys but that small, potentially important functional differences exist.

cortex | marmoset | functional MRI | naturalistic movie

The common marmoset has become an important nonhuman primate model for bridging the translational gap between rodents and humans. Marmosets have a lissencephalic cortex, like rodents, but as primates, they possess a complex visual system (1) and exhibit a similar visuomotor behavior as macaques and humans (2, 3). This, paired with a high reproductive power, small size, and fast maturation rate, make this nonhuman primate (NHP) species particularly interesting for neuroscience.

To identify and compare the functional architecture of the primate brain, functional MRI (fMRI) has often been applied because of its noninvasive measures and whole brain coverage (4, 5). In particular, resting-state fMRI (RS-fMRI) has been used 1) to identify homologous large-scale brain networks between marmosets and humans (6, 7), 2) to define functional boundaries based on intrinsic functional connectivity (8, 9), and 3) to use functional connectivity "fingerprints" of brain areas to establish similarities between marmosets, rodents, and humans (10). Because resting-state patterns are state agnostic and spontaneous, however, this technique cannot be used to map the functional correspondences of interspecies blood oxygen level–dependent (BOLD) fluctuations over time. Task-based fMRI is better suited for mapping stimuli-driven fluctuations across species, and, indeed, a few studies have used task-based fMRI in awake marmosets to identify areas related to specific functions [e.g., visuosaccadic orienting (11), processing of faces and bodies (12, 13), looming and receding visual stimuli (14), and tactile processing (15)]. A major drawback of task-based fMRI is that compliance is often poor in NHPs and that each task can only reveal the limited set of functional activations for which it was designed.

These limitations can be overcome by employing movie stimuli, which provide rich and naturalistic stimulations. Human studies have shown that movie-driven fMRI (md-fMRI) responses are highly selective between brain regions, engage many brain regions, and are highly reliable between subjects (16–19). Functional correspondences between species can be directly tested by the interspecies activity correlation (ISAC) method, which uses the md-fMRI time course in a seed region in one species to identify functional correspondences across the cortex of the other species. This technique has been successfully employed to identify functional correspondences (analogies) between human and macaque cortical areas (20), but this powerful mapping technique has yet to be applied to the marmoset brain.

Here, we used md-fMRI to compare directly the brain activations between marmosets and humans and to establish functional correspondences between cortical areas across the brain in the two species. We focused our analysis on identifying analogies of the well-known human face-, body-, and scene-selective networks in the marmoset brain. Not only do these networks play pivotal roles in complex primate vision, face- and body-selective areas have also been described by a few task-based fMRI studies in marmosets (12, 13), providing an independent validation for some of these results.

Significance

The common marmoset has enormous promise as a nonhuman primate model. While resting-state functional MRI (fMRI) has provided evidence for a similar organization of marmoset and human cortices, the technique cannot be used to map the functional correspondences of brain regions between species. Here, we used movie-driven fMRI in marmosets and humans to identify whole-brain functional correspondences between the two primate species. In particular, we describe functional correlates for the well-known human face, body, and scene patches in marmosets. We find that these networks have a similar organization in both species, suggesting a largely conserved organization of higher-order visual areas between marmoset monkeys and humans.

Author contributions: Y.H. and S.E. designed research; Y.H., J.C.C., J.S., K.D.J., and S.E. performed research; Y.H. analyzed data; and Y.H., J.C.C., D.J.S., K.D.J., R.S.M., and S.E. wrote the paper.

The authors declare no competing interest.

This article is a PNAS Direct Submission.

[1]To whom correspondence may be addressed. Email: yhori@uwo.ca or severlin@uwo.ca.

This article contains supporting information online at https://www.pnas.org/lookup/suppl/doi:10.1073/pnas.2110980118/-/DCSupplemental.

Published September 7, 2021.

Results

A total of 13 human participants and eight marmoset monkeys freely watched a 15-min naturalistic movie with no sound. The movie was selected to keep marmosets interested and showed a fictitious day of a marmoset living in and navigating through an urban environment. Aside from marmosets (present in ∼57% of the movie), a variety of other species (humans, owls, capybaras, dogs, cats, pigeons, roosters, frogs, and ants) are also present in some parts (∼27%). The movie was presented once to each human participant and one to four times to each monkey on separate days.

Intersubject Variability of the Stimulus-Driven Activity. We first identified the cortical brain regions with consistent md-fMRI activity among subjects to remove the low reproducible areas from the subsequent analysis. To this end, we calculated intersubject correlation maps for the human and marmoset participants. We found high correlations between subjects in occipital, temporal, and parietal areas in both species (Fig. 1 *A*–*F* and *SI Appendix*, Fig. 1 *A*–*D* for the right hemisphere). Unlike humans, marmosets also showed high correlations in prefrontal cortices (PFC) including the medial PFC (mPFC; A25, A32), ventrolateral PFC (vlPFC; A45, A47), and dorsomedial PFC (dmPFC; A8b, A9). These findings are very similar to a previous human and macaque monkey study (20). A difference from this previous study is a lack of correlations in human auditory areas because our subjects watched the movie with no sound.

Intra- and Interspecies Functional Correspondence. To identify the intra- and interspecies functional correspondence in early and high-order visual areas, we created the volume-of-interests (VOIs) based on the intersubject correlation maps using the multimodal cortical parcellation atlas (21) for humans and the Paxinos atlas for marmosets (22) (Fig. 1 *G* and *H* and *SI Appendix*, Fig. 1 *E* and *F* for the right VOIs). The time courses were extracted from all VOIs, and cross-correlation coefficients were calculated between all human and marmoset VOIs (Fig. 1*I* and *Methods*). The correlation matrices are shown in *SI Appendix*, Fig. 2. We found similar functional responses in human face- and known marmoset face-specific areas. For example, we found functional similarities between the fusiform face complex (FFC) and posterior inferotemporal areas (PIT) (21, 23–26) in humans and the V4 transitional part (V4T), fundal superior temporal area (FST), and TE3 in marmosets. The human peri-entorhinal and ectorhinal cortex (PeEc) was also correlated with the marmoset TE3. These marmoset areas are known to correspond to face patches based on blocked fMRI tasks (12, 13).

Identification of Marmoset Areas Corresponding to Human Face-, Body-, and Scene-Specific Areas. As a validation of our method, we next asked whether the previously described marmoset face patches (12, 13) could be detected by comparing the time courses across the marmoset brain to the time course in one of the human face patches, PeEc (21), also known as the anterior face patch or Brodmann area 35/36 (23, 26). Calculating the cortex-wise correlation with the time course in the human face patch revealed discrete patches of the activity in both human (red regions in Fig. 2 *A* and *C*) and marmoset occipital and temporal areas (red regions in Fig. 2 *B* and *D*). There were four main clusters in temporal areas (*SI Appendix*, Tables 1 and 2 for humans and marmosets, respectively). Each cluster (F1, F2, F3, and F4) in humans consisted of PeEc and TF for F1, FFC and PH, the TE2 posterior area (TE2p) for F2, LO2, and PIT, V4T for F3, and the middle temporal area (MT) and medical superior temporal area (MST) for F4 (Fig. 2*C*). Each cluster (F1, F2, F3, and F4) in marmosets consisted of area 36 (A36) and the entorhinal cortex (Ent) for F1, TE3 and the temporo-parieto-occipital association area for F2, FST and Pga-IPa for F3, and MT, MST, and V4T for F4 (Fig. 2*C*). The locations of these patches closely resembled those reported in the previous macaque (26–30) and marmoset fMRI studies (12, 13), but we also found statistically significant activation in marmoset A36. This area has not been found in previous marmoset face fMRI studies, but it cytoarchitectonically corresponds to the anterior face patch in humans (21, 23, 26, 31). These marmoset areas were also found when we used the other human face patches, FFC and PIT, as seed regions (*SI Appendix*, Fig. 5). This mapping of the face patches under more naturalistic viewing conditions demonstrates that it is possible to use this approach to identify marmoset areas that have the same function as specific human areas. All marmoset correlation coefficient maps with human VOIs are shown in *SI Appendix*, Figs. 3–6, and the peak locations of these maps are summarized in Fig. 3.

Next, we sought to examine which marmoset areas correspond to body- and scene-specific areas in humans. To do so, we seeded the human TE2p (21) and parieto-occipital sulcus area 1 [POS1 (21, 32)], also known as the retrosplenial cortex (33), to identify marmoset body- and scene-specific areas, respectively. Body-specific areas have already been described in one previous blocked fMRI study in marmosets (13), and these areas are located adjacent to face patches, as in humans and macaque monkeys (29, 34, 35). Scene-specific areas have not yet been identified in marmosets.

The time course in the human body-specific area (TE2p) was highly correlated with parts of face-specific areas (FFC and PIT) and the posterior superior temporal sulcus in humans, which is known as one of the body patches (35) (blue regions in Fig. 2 *A* and *C* and *SI Appendix*, Table 1). The time course in the human body patch was also highly correlated with the areas adjacent to the face patches in marmosets (blue regions in Fig. 2*B* and *D* and *SI Appendix*, Table 2).

The time course in the human scene-specific area (POS1) was highly correlated with A31, the dorsal visual transitional area, the PG posterior part, the parahippocampal area (PHA), the prostriate area (ProSt), the ventromedial visual area (VMV), V1, V2, and V3 in humans (green regions in Fig. 2 *A* and *B* and *SI Appendix*, Table 1), and area 19 of medial part (A19M), ProSt, TH (also known as PHA), V1, V2, and V3 in marmosets (green regions: Fig. 2 *C* and *D* and *SI Appendix*, Table 2). The locations of scene-specific areas in humans closely resembled those reported in previous human studies (36–39). The activation areas in marmosets were broadly cytoarchitectonically consistent with human activation areas.

To identify cortical areas with similar BOLD time courses in humans and marmosets, we computed for each human VOI the correlation of its time course with all marmoset cortical voxels and then plotted the peak locations of these correlation maps on the marmoset brain surface (Fig. 3). Although human and marmoset regions do not always correspond directly based on cytoarchitecture, we could clearly identify regions with similar time courses between the two species. Human face-specific areas (FFC and PIT), for example, have a similar time course to marmoset area V4T (red point in Fig. 3*B*), and the human scene-specific area POS1 has a similar time course as the PHA TH in marmosets (light blue point in Fig. 3*B*).

Relative Contribution of Different Features in Face Patches. To evaluate what features in the movie activate marmoset regions functionally corresponding to human face and body patches, we first identified, for each repetiton time (TR) interval (1.5 s) of the movie, whether a marmoset, other animals (humans, owls, capybaras, dogs, cats, pigeons, roosters, frogs, scorpions, and ants), or no animals were visible. These three pseudoevent-related designs were convolved with a hemodynamic response function using FSL FEAT (Fig. 4*A*). We then calculated the correlation coefficients between these predicted designs and the time courses in each face and body patch. We found that the human face patches were more active when

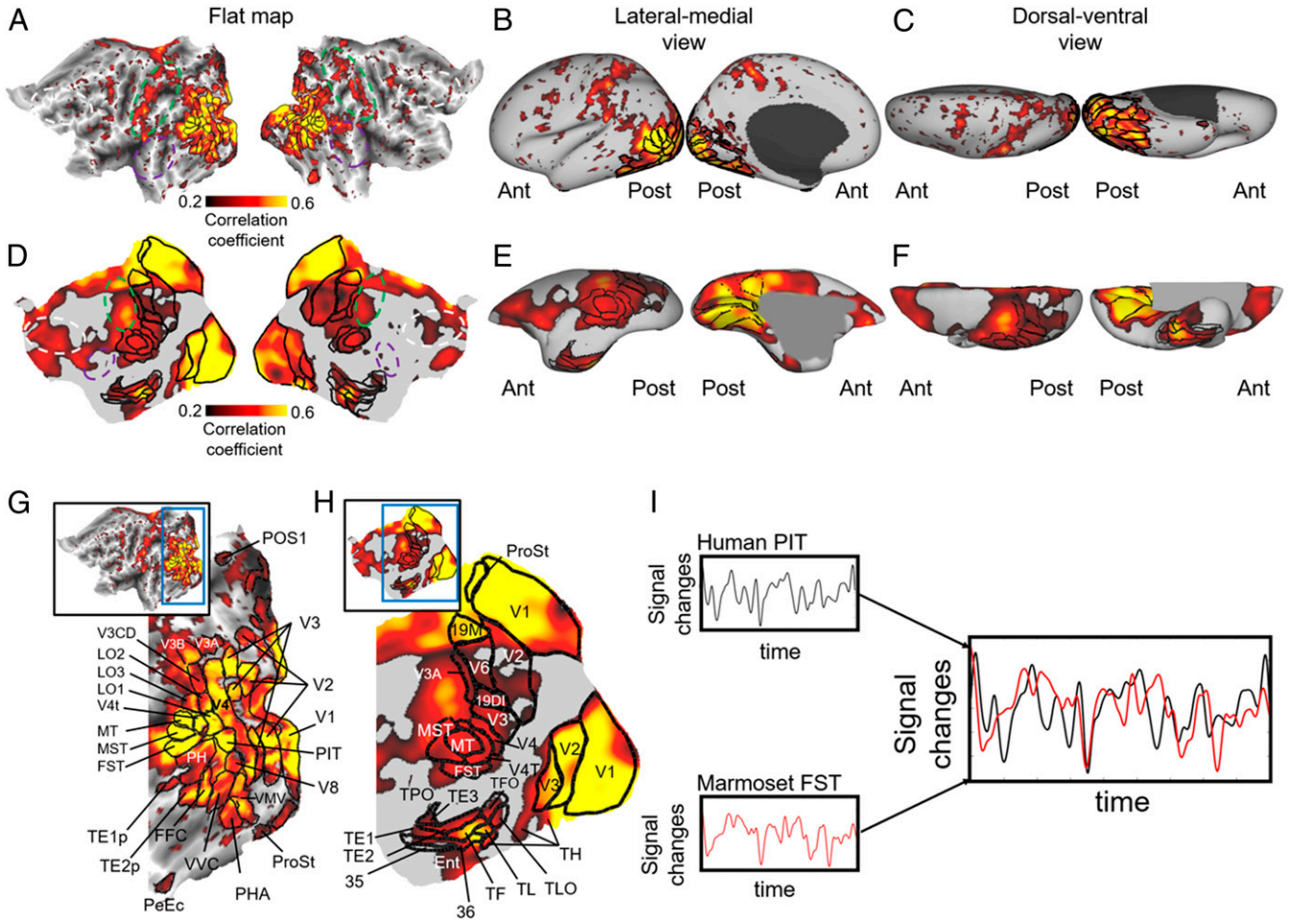

Fig. 1. Intersubject correlation map of brain activity during movie viewing. Spatial maps of correlated brain activity across 13 human subjects (*A*–*C*) and eight marmoset subjects (*D*–*F*), mapped on each flattened cortex (*A* and *D*) and left cortical surface [lateral-medial view (*B* and *E*) and dorsal-ventral view (*C* and *F*)]. Approximate locations of parietal, auditory, and frontal regions are indicated by green, purple, and white dashed lines on the flat maps, respectively. The VOIs in visual-related areas were manually created based on the multimodal cortical parcellation atlas (21) for humans and Paxinos atlas for marmosets (22) so as not to include the low correlation areas among scans (*G* for humans and *H* for marmosets). Then, the time courses were extracted from two VOIs (e.g., PIT in humans and FST in marmosets), and the cross-correlation coefficient was calculated between them (*I*). See *SI Appendix*, Fig. S1 for the right hemisphere. LO1-3: area lateral occipital 1 to 3; VVC: ventral visual complex; A19DI: area 19 of cortex dorsointermediate part; TLO: temporal area TL occipital part; TPO: temporo-parieto-occipital association area.

they watched not only marmosets but also the other animals compared to no animals (Fig. 4*B*; $P < 0.05$ for cluster F1, $P < 0.01$ for clusters F2, F3, and F4; ANOVA with Bonferroni post hoc correction). This tendency was also found for the human body patches (Fig. 4*B*; $P < 0.01$ for cluster B1; paired t test with Bonferroni post hoc correction). Unlike humans, marmoset face patches were more active when they watched marmosets (Fig. 4*C*; $P < 0.05$ for cluster F2, $P < 0.01$ for cluster F4; ANOVA with Bonferroni post hoc correction) than when they watched the other animals. As in humans, the marmoset body patches were activated when they watched both marmosets and the other animals compared to no animals (Fig. 4*B*; $P < 0.05$; paired t test with Bonferroni post hoc correction).

Identification of Human Areas Corresponding to Marmoset Parietal Areas. As shown in Fig. 1, both human and marmoset parietal areas also had high reproducibility between scans. We next asked which marmoset areas correspond to each human parietal area using the same method as high-order visual areas. However, for most human parietal areas, we could not find correlations with parietal areas in marmosets (*SI Appendix*, Figs. 7–8). Therefore, we next identified human parietal areas that correlated with each marmoset area surrounding the intraparietal sulcus (IPS) (the anterior intraparietal parietal area [AIP], lateral intraparietal parietal area [LIP], medial intraparietal area [MIP], PE, PG, occipito-parietal transitional area [OPt], and the ventral parietal area [VIP]). The analysis showed that the peak locations of the human correlation maps were located in the area PG inferior part (PGi) for the marmoset anterior/ventral parietal regions (AIP, OPt, PE, and PG) and in the human area PG superior part (PGs) for the marmoset parietal regions LIP, MIP, and VIP (Fig. 5).

Discussion

In this study, we aimed to identify areas in the marmoset that functionally correspond to high-order visual areas in humans, in particular face-, body-, and scene-specific areas. To do so, we presented human participants and marmoset monkeys with a naturalistic movie during fMRI acquisition at ultra-high field. We found functional responses in human face patches (i.e., PeEc, FFC, and PIT) that were in good agreement with those in marmoset dorsal face patches (12, 13) (i.e., an anterior dorsal [AD], a middle dorsal [MD], and a posterior dorsal [PD] area). In addition, we observed a

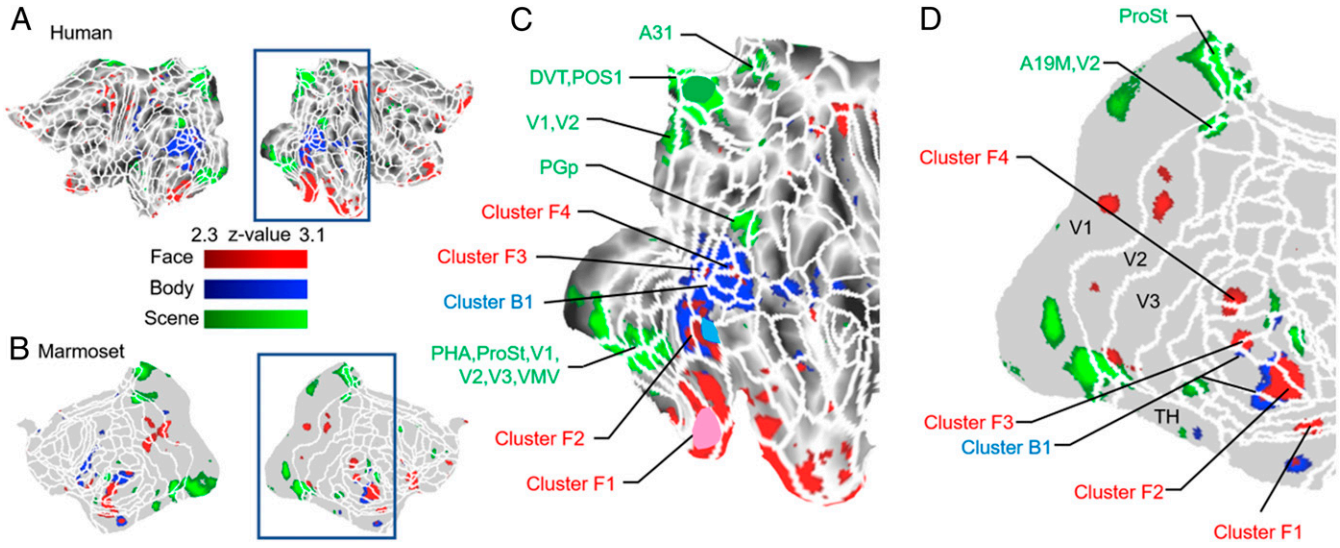

Fig. 2. Correlation maps (z-score maps) in human (*A*) and marmoset (*B*) brains with human face-specific (PeEc indicated by pink area in *C*), body-specific (TE2p indicated by light blue area in *C*), and scene-specific (POS1 indicated by green area in *C*) areas in the right hemisphere were presented on each flattened map. *C* and *D* show the same data focusing around the occipital and temporal regions (areas surrounded by blue squares in *A* and *B*) in right hemispheres. White lines indicate the borders of the multimodal cortical parcellation atlas (21) for humans and the Paxinos atlas for marmosets (22). The correlation coefficient maps with human VOIs in the left hemisphere are shown in *SI Appendix*, Figs. 3–6.

functional correspondence between the PeEc in humans and area 36 in marmosets, which had not yet been described in previous studies. The human PeEc in the multimodal parcellation atlas (21) corresponds to the anterior face patch (AFP) and Brodmann area 36 (21, 23, 26, 31). Thus, area 36 in marmosets seems to correspond to the AFP in humans. We also found a small asymmetry between the left and right hemisphere in marmosets, but we believe that this difference was likely caused by differences in the coil sensitivity as shown in our previous studies (7, 40). To further explore the functions of marmoset face patches, we also identified what features in the movie activated the different patches. These analyses demonstrated that face patches in marmosets responded to marmosets but not other animals, whereas human face patches exhibited similar responses to marmosets and other animals. This tendency was similar to a previous NHP study in macaques that showed that macaque face patches responded more than twice as strongly to macaque faces compared to human faces, whereas human face patches responded similarly to the presentation of both human and macaque faces (29). This indicates that both macaque and marmoset face patches preferentially respond to conspecific faces.

Previous systematic mapping of human and macaque visual cortices onto each other have revealed an overall shift of areas ventrally from the superior temporal sulcus (STS) in humans compared to macaque monkeys (41), corresponding to an overall areal expansion in this region (42). Along with this shift of face areas, macaque face patches are located more dorsally compared to human face patches (26). As in macaque monkeys, marmoset face patches are also located dorsally compared to human face patches (12, 13). Given the locations of marmoset face patches relative to each other, the marmoset AD and MD face patches along the marmoset STS (corresponding to the clusters F2 and F3 in Fig. 2*D*) are in a similar position as the macaque anterior fundus and middle fundus face patches, respectively (26). Their positions also bear a resemblance to two face patches in the anterior and posterior STS in humans (43, 44), although the correspondence between the human and nonhuman primate is still a matter of speculation (45). The marmoset PD patch (corresponding to the cluster F4 in Fig. 2*D*), which is located in MT, MST, and V4T, is in a similar position as posterior lateral (PL) in macaque V4T (46) and an occipital facial area in human PIT (26, 47). On the other hand, we could not detect ventral face patches in marmosets [i.e., posterior ventral and middle ventral (12, 13)]. The face patches along the dorsoventral axis show different selectivity to natural motion (48, 49). Ventral face patches have a preference for rapidly varying face stimuli, whereas dorsal face patches have a preference for natural motion. These differences in selectivity may present the detection of ventral face patches with the movie employed here.

Body and Scene Patch Systems in Humans and Marmosets. The functional responses in the human body-specific patch (TE2p) were in good agreement with those in the marmoset area located adjacent to MD. This area is already known as a marmoset body-specific patch based on a previous electrocorticography and fMRI study (13). In addition, we also found that the human TE2p correlated with the marmoset area adjacent to the anterior part of AD, which had not been found yet. This finding is broadly consistent with previous findings in macaques and humans of body-selective areas located adjacent to face patches (29, 34, 50–53).

In humans, previous fMRI studies (29, 50, 51, 53) have described three visual cortical regions that are more active during the presentation of scenes or isolated houses compared with the presentation of other visual stimuli such as faces, objects, body parts, or scrambled scenes. Typically, these human brain regions are located in POS1, PHA, and transverse occipital sulcus. In this study, we found that functional responses in human POS1 and PHA corresponded to those in the marmoset retrosplenial cortex (A19M) and in the parahippocampal area (TH), suggesting a homologous neural architecture for scene-selective regions in the visual cortex for humans and marmosets.

Functional Correspondence in Parietal and Motion-Selective Visual Areas. We identified areas in the marmoset that functionally corresponded to face-, body-, and scene-specific areas in humans. Next, we sought to examine which marmoset areas show functional correspondences to other visual areas in humans. Our results demonstrate that the area MT and its surrounding areas in humans (FST, LO1, LO2, LO3, MST, and V4T) corresponded to a region at the border between FST, MST, and V4T. The area MT in both New- and Old-World monkeys has direction-selective neurons (54)

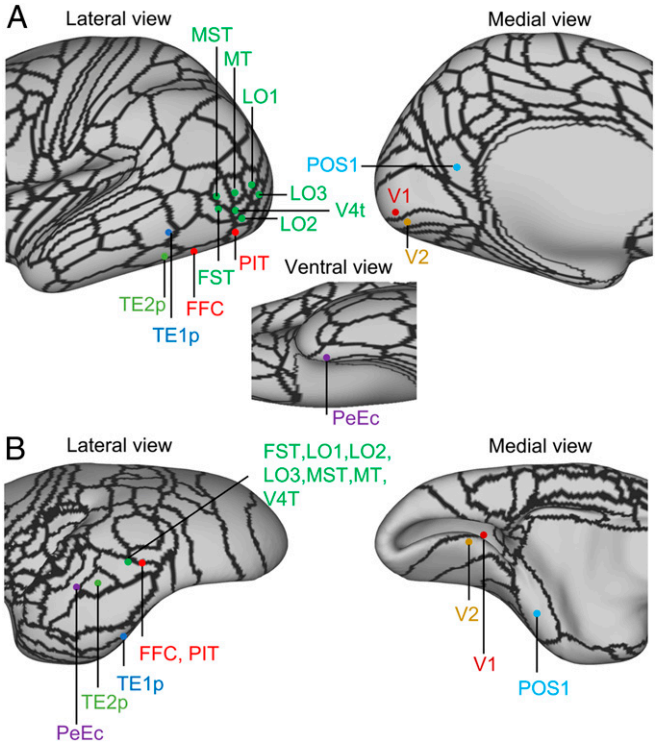

Fig. 3. The peak locations of human (*A*) and marmoset (*B*) correlation maps with the time course in each human VOI (presented by color labels). Note that 11 out of 26 human VOIs (V3, V3A, V3B, V3CD, V4, V8, PH, PHA, ProSt, VMV, and VVC) were not presented due to the differences of the peak locations between the left and right hemispheres. The maps were focused on the areas around the occipital and temporal regions in the left hemispheres. Black lines indicate the borders of the multimodal cortical parcellation atlas (21) for humans and the Paxinos atlas for marmosets (22).

and is considered to play an important role in motion perception, direction selectivity, and speed turning (55–57). The major output of MT is in the cortical areas surrounding it (i.e., FST, MST, and V4T) (see ref. 58 for macaques and ref. 59 for marmosets). Therefore, the movie may not be suitable to identify small functional differences between these regions. The movie we used was selected to identify face, body, and scene patches. To better identify motion-related areas, it would be ideal to use a movie in which stimuli move in various directions, speeds, and rotations, but this is beyond the scope of this study.

Although we could not identify functional differences between most marmoset parietal areas, the anterior/ventral (AIP, OPt, PE, and PG) and parietal regions surrounding the IPS (LIP, MIP, and VIP) in marmosets were correlated with PGi and PGs, respectively. As described in numerous studies, human PG is a part of the default mode network (DMN), while the areas surrounding the IPS (e.g., area LIP) is a part of the attention network (ATN) (21, 60, 61). In addition, the time courses of BOLD signals in human PG are anticorrelated with those in task positive regions (e.g., frontal eye field and LIP) even under resting state (62). In marmosets, one of the core regions of the DMN is the cortex surrounding the IPS (6, 63, 64). A functional imaging study in marmosets showed that these areas were deactivated during a visual stimulation task relative to the period when a black screen was presented (64). On the other hand, the area surrounding the marmoset IPS have also been linked to the attention-like frontoparietal network by several RS-fMRI studies (6, 65). It is also known that electrical microstimulation in the areas surrounding the IPS evoke saccadic eye movements (65) and that single neurons in the region show neural correlates for the gap effect in saccadic eye movement tasks (66). As such, it seems that parietal areas surrounding the IPS in the marmoset are involved in both default mode and ATNs. Taken together with our finding that the marmoset parietal area corresponded to the parietal regions in the human DMN, the DMN might be predominantly engaged during movie viewing in the marmoset. Indeed, our results showed that the human PG was correlated with the posterior cingulate cortex, dorsolateral prefrontal cortex, and parts of the anterior cingulate cortex and temporal areas (*SI Appendix*, Fig. 9) and that these areas overlap with the human DMN (21, 60, 61), which is deactivated during attention-demanding tasks (62, 67). Note that standardized cytoarchitectonic borders (as in the Paxinos atlas we used) may not always be accurate for each subject. Indeed, a recent paper showed that the location of marmoset LIP exhibits substantial variability across subjects (68).

Differences between Human and Marmoset Frontal Areas. We also observed consistent activation in marmoset frontal areas, in particular, the mPFC (A25, A32), vlPFC (A45, A47), and dmPFC (A8b, A9) (Fig. 1 *D*–*F*). This distribution closely resembled a recently identified network for social interaction processing (40, 69). We found that the macaque mPFC, vlPFC, and dmPFC are more activated when the monkey watched a social video (in which two monkeys were interacting with each other) compared to a nonsocial video (in which two monkeys were separately acting in their own environment). As such, consistent activation in the marmoset frontal areas might reflect social interaction processing during movie viewing. Although humans possess a similar social interaction network (70, 71), the social interactions of marmosets might not have been enough to consistently activate this network in our human participants.

Conclusion

In summary, we identified marmoset areas that functionally corresponded to human face-, body-, and scene-processing areas using md-fMRI. The locations of these marmoset areas relative to each other were broadly consistent with those of human areas, suggesting that high-order visual processing might be a conserved feature between humans and New World marmoset monkeys. These findings further strengthen the marmoset as a powerful nonhuman primate model for visual and social neuroscience.

Methods

Subjects. A total of 13 healthy volunteers (nine males and four females, 22 to 56 y) and eight common marmosets (six males and two females, 20 to 42 mo, 300 to 436 g) participated in this study. All surgical and experimental procedures for marmosets were in accordance with the Canadian Council of Animal Care policy and a protocol approved by the Animal Care Committee of the University of Western Ontario Council on Animal Care. All animal experiments complied with the Animal Research: Reporting In Vivo Experiments guidelines. Human volunteers were informed about the experimental procedures and provided informed written consent. This study was approved by the Ethics Committee of the University of Western Ontario.

Experimental Setup. All marmosets underwent surgery to implant a head chamber to immobilize the head during MRI acquisition as described in previous reports (7, 72) and were trained to acclimatize to the MRI scanning environment and head-fixation system. Both humans and marmosets watched a 15-min naturalistic movie with no sound. The movie was edited from the British Broadcasting Corporation episode "Urban Jungles" from the "Hidden Kingdoms" series. The episode was condensed to 15 min by removing the parts that were not related to marmosets living in Rio de Janeiro and removing some scenes that seemed to be less interesting to marmosets based on some pilot data (essentially scenes that did not show any marmosets for a while).

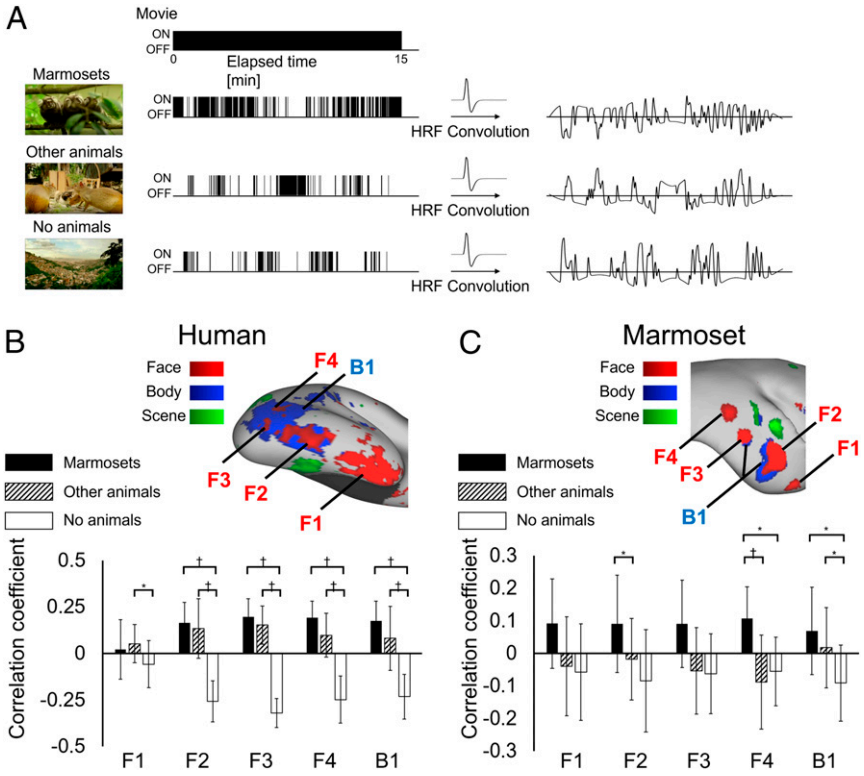

Fig. 4. Correlations of the time course in each face or body patch with the pseudoevent-related design. We first identified which animals (marmosets, other animals, or no animals) we can find in each TR (1.5 s) in the movie clip, and they were classified as 0 (OFF) and 1 (ON). These pseudoevent-related designs were convolved by hemodynamic response function and were applied as regressors of interest (*A*). Correlation coefficients between the predicted designs and the time courses in each face and body patch in human (*B*) and marmoset (*C*). The locations of the clusters are shown on the cortical surfaces (F1 to F4 for face-specific clusters and B1 for body-specific clusters), which is the same data as shown in Fig. 2 *C* and *D*. The black, slash, and white bars indicate the correlation coefficient values with the features of marmosets, other animals, and no animals, respectively. An asterisk and a cross indicate significant differences of $P < 0.05$ and $P < 0.01$ using ANOVA with Bonferroni post hoc correction, respectively. Error bars indicate the SDs.

MRI Acquisition. Human volunteers lay in a supine position and watched the movie presented via a rear projection system (Avotech SV-6011, Avotec Incorporated) through a surface mirror affixed to head coil (6.9° field of view from the center to the side of the screen). Each marmoset was fixed to the animal holder using a neck plate and a tail plate. The marmoset was then head-fixed in a sphinx position using fixation pins in the MRI room to minimize the time in which the awake animal was head fixed (7). In marmosets, the eyes were monitored using an MRI-compatible camera (Model 12M-i, MRC Systems GmbH) to make sure that the animals stayed awake. For both species, the movie was presented via Powerpoint on a MacBook Pro.

Human images were acquired using a 68-cm head-only 7 T MRI scanner (Siemens Magnetom 7T MRI Plus) with an AC-84 Mark II gradient coil, an in-house 8-channel parallel transmit, and a 32-channel receive coil (73). Marmoset images were acquired using a 9.4 T 31-cm horizontal bore magnet (Varian/Agilent) and Bruker BioSpec Avance III HD console with the software package Paravision-6 (Bruker BioSpin Corp), a custom-built high-performance 15-cm-diameter gradient coil with 400-mT/m maximum gradient strength (74), and the five-channel receive coil (7). Full details of acquisition and analysis procedures can be found in *SI Appendix*.

Data Analysis. To estimate the intersubject variability of stimulus-driven activity, we calculated the voxel-by-voxel correlation across subjects within each species after preprocessing the fMRI datasets such as motion correction, distortion correction, and normalization to the template. The time courses were extracted from each VOI (26 and 25 VOIs for humans and marmosets, respectively), and intra- and interspecies correlation matrices were created by cross-correlating the time courses among two regions using Matlab (MathWorks). To identify marmoset areas that have similar functional activations as human visual-related regions, we extracted the human time course in each 26 VOI, and we created the correlation coefficient maps with these time courses. These correlation coefficient maps were Fisher Z-transformed for each of the two species and were thresholded at z = 2.3. Full details of acquisition and analysis procedures can be found in *SI Appendix*.

Data Availability. Data and code are available on GitHub, https://github.com/everlingmarmoset/moviedriven-fMRI (75). The movie we used here is available via email upon request due to commercial copyrights: severlin@uwo.ca. All other study data are included in the article and/or *SI Appendix*.

ACKNOWLEDGMENTS. This work was supported by the Canadian Institutes of Health Research (FRN 148365, FRN 353372) and the Canada First Research Excellence Fund to BrainsCAN. We also thank Miranda Bellyou, Cheryl Vander Tuin, and Hannah Pettypiece for animal preparation and care and Dr. Alex Li and Trevor Szekeres for scanning assistance.

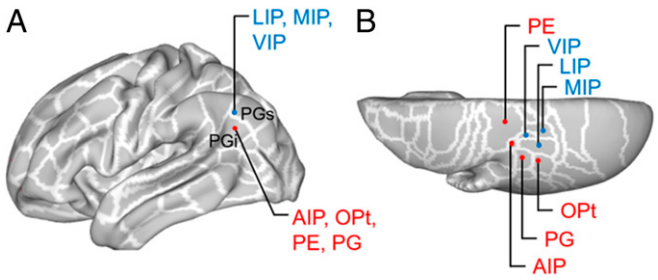

Fig. 5. The peak locations of human (*A*) and marmoset (*B*) correlation maps with the time course in each marmoset parietal VOI (presented by red or blue labels). White lines indicate the borders of the multimodal cortical parcellation atlas (21) for humans and the Paxinos atlas for marmosets (22).

1. S. G. Solomon, M. G. P. Rosa, A simpler primate brain: the visual system of the marmoset monkey. *Front. Neural Circuits* **8**, 96 (2014).
2. J. F. Mitchell, D. A. Leopold, The marmoset monkey as a model for visual neuroscience. *Neurosci. Res.* **93**, 20–46 (2015).
3. C.-Y. Chen *et al*., Properties of visually guided saccadic behavior and bottom-up attention in marmoset, macaque, and human. *J. Neurophysiol.* **125**, 437–457 (2021).
4. M. P. Milham *et al*., An open resource for non-human primate imaging. *Neuron* **100**, 61–74.e2 (2018).
5. M. Milham *et al*., Accelerating the evolution of nonhuman primate neuroimaging. *Neuron* **105**, 600–603 (2020).
6. Y. Hori *et al*., Altered resting-state functional connectivity between awake and isoflurane anesthetized marmosets. *Cereb. Cortex* **30**, 5943–5959 (2020).
7. D. J. Schaeffer *et al*., Integrated radiofrequency array and animal holder design for minimizing head motion during awake marmoset functional magnetic resonance imaging. *Neuroimage* **193**, 126–138 (2019).
8. D. J. Schaeffer *et al*., Intrinsic functional clustering of anterior cingulate cortex in the common marmoset. *Neuroimage* **186**, 301–307 (2019).
9. D. J. Schaeffer, K. M. Gilbert, J. S. Gati, R. S. Menon, S. Everling, Intrinsic functional boundaries of lateral frontal cortex in the common marmoset monkey. *J. Neurosci.* **39**, 1020–1029 (2019).
10. D. J. Schaeffer *et al*., Divergence of rodent and primate medial frontal cortex functional connectivity. *Proc. Natl. Acad. Sci. U.S.A.* **117**, 21681–21689 (2020).
11. D. J. Schaeffer *et al*., Task-based fMRI of a free-viewing visuo-saccadic network in the marmoset monkey. *Neuroimage* **202**, 116147 (2019).
12. D. J. Schaeffer *et al*., Face selective patches in marmoset frontal cortex. *Nat. Commun.* **11**, 4856 (2020).
13. C. C. Hung *et al*., Functional mapping of face-selective regions in the extrastriate visual cortex of the marmoset. *J. Neurosci.* **35**, 1160–1172 (2015).
14. J. C. Cléry *et al*., Looming and receding visual networks in awake marmosets investigated with fMRI. *Neuroimage* **215**, 116815 (2020).
15. J. C. Cléry *et al*., Whole brain mapping of somatosensory responses in awake marmosets investigated with ultra-high-field fMRI. *J. Neurophysiol.* **124**, 1900–1913 (2020).
16. U. Hasson, O. Furman, D. Clark, Y. Dudai, L. Davachi, Enhanced intersubject correlations during movie viewing correlate with successful episodic encoding. *Neuron* **57**, 452–462 (2008).
17. U. Hasson, R. Malach, D. J. Heeger, Reliability of cortical activity during natural stimulation. *Trends Cogn. Sci.* **14**, 40–48 (2010).
18. Y. Lerner, C. J. Honey, L. J. Silbert, U. Hasson, Topographic mapping of a hierarchy of temporal receptive windows using a narrated story. *J. Neurosci.* **31**, 2906–2915 (2011).
19. L. Naci, R. Cusack, M. Anello, A. M. Owen, A common neural code for similar conscious experiences in different individuals. *Proc. Natl. Acad. Sci. U.S.A.* **111**, 14277–14282 (2014).
20. D. Mantini *et al*., Interspecies activity correlations reveal functional correspondence between monkey and human brain areas. *Nat. Methods* **9**, 277–282 (2012).
21. M. F. Glasser *et al*., A multi-modal parcellation of human cerebral cortex. *Nature* **536**, 171–178 (2016).
22. G. Paxinos, C. Watson, M. Petrides, M. G. P. Rosa, H. Tokuno, *The Marmoset Brain in Stereotaxic Coordinates* (Academic Press, 2012).
23. J. C. Augustinack *et al*.; Alzheimer's Disease Neuroimaging Initiative, Predicting the location of human perirhinal cortex, Brodmann's area 35, from MRI. *Neuroimage* **64**, 32–42 (2013).
24. I. Gauthier *et al*., The fusiform "face area" is part of a network that processes faces at the individual level. *J. Cogn. Neurosci.* **12**, 495–504 (2000).
25. N. Kanwisher, J. McDermott, M. M. Chun, The fusiform face area: a module in human extrastriate cortex specialized for face perception. *J. Neurosci.* **17**, 4302–4311 (1997).
26. D. Y. Tsao, S. Moeller, W. A. Freiwald, Comparing face patch systems in macaques and humans. *Proc. Natl. Acad. Sci. U.S.A.* **105**, 19514–19519 (2008).
27. J. K. Hesse, D. Y. Tsao, The macaque face patch system: a turtle's underbelly for the brain. *Nat. Rev. Neurosci.* **21**, 695–716 (2020).
28. S. M. Landi, W. A. Freiwald, Two areas for familiar face recognition in the primate brain. *Science* **357**, 591–595 (2017).
29. D. Y. Tsao, W. A. Freiwald, T. A. Knutsen, J. B. Mandeville, R. B. H. Tootell, Faces and objects in macaque cerebral cortex. *Nat. Neurosci.* **6**, 989–995 (2003).
30. K. S. Weiner, K. Grill-Spector, The evolution of face processing networks. *Trends Cogn. Sci.* **19**, 240–241 (2015).
31. R. Rajimehr, J. C. Young, R. B. H. Tootell, An anterior temporal face patch in human cortex, predicted by macaque maps. *Proc. Natl. Acad. Sci. U.S.A.* **106**, 1995–2000 (2009).
32. M. F. Glasser, D. C. Van Essen, Mapping human cortical areas in vivo based on myelin content as revealed by T1- and T2-weighted MRI. *J. Neurosci.* **31**, 11597–11616 (2011).
33. S. Nasr *et al*., Scene-selective cortical regions in human and nonhuman primates. *J. Neurosci.* **31**, 13771–13785 (2011).
34. M. V. Peelen, P. E. Downing, The neural basis of visual body perception. *Nat. Rev. Neurosci.* **8**, 636–648 (2007).
35. M. A. Pinsk *et al*., Neural representations of faces and body parts in macaque and human cortex: a comparative FMRI study. *J. Neurophysiol.* **101**, 2581–2600 (2009).
36. G. K. Aguirre, E. Zarahn, M. D'Esposito, An area within human ventral cortex sensitive to "building" stimuli: evidence and implications. *Neuron* **21**, 373–383 (1998).
37. R. Epstein, N. Kanwisher, A cortical representation of the local visual environment. *Nature* **392**, 598–601 (1998).
38. A. Ishai, L. G. Ungerleider, J. V. Haxby, Distributed neural systems for the generation of visual images. *Neuron* **28**, 979–990 (2000).
39. E. A. Maguire, Studying the freely-behaving brain with fMRI. *Neuroimage* **62**, 1170–1176 (2012).
40. J. C. Cléry, Y. Hori, D. J. Schaeffer, R. S. Menon, S. Everling, Neural network of social interaction observation in marmosets. *eLife* **10**, e65012 (2021).
41. G. A. Orban, D. Van Essen, W. Vanduffel, Comparative mapping of higher visual areas in monkeys and humans. *Trends Cogn. Sci.* **8**, 315–324 (2004).
42. D. C. Van Essen, D. L. Dierker, Surface-based and probabilistic atlases of primate cerebral cortex. *Neuron* **56**, 209–225 (2007).
43. J. D. Carlin, A. J. Calder, N. Kriegeskorte, H. Nili, J. B. Rowe, A head view-invariant representation of gaze direction in anterior superior temporal sulcus. *Curr. Biol.* **21**, 1817–1821 (2011).
44. D. Pitcher, D. D. Dilks, R. R. Saxe, C. Triantafyllou, N. Kanwisher, Differential selectivity for dynamic versus static information in face-selective cortical regions. *Neuroimage* **56**, 2356–2363 (2011).
45. G. Yovel, W. A. Freiwald, Face recognition systems in monkey and human: are they the same thing? *F1000Prime Rep.* **5**, 10 (2013).
46. T. Janssens, Q. Zhu, I. D. Popivanov, W. Vanduffel, Probabilistic and single-subject retinotopic maps reveal the topographic organization of face patches in the macaque cortex. *J. Neurosci.* **34**, 10156–10167 (2014).
47. R. O. Abdollahi *et al*., Correspondences between retinotopic areas and myelin maps in human visual cortex. *Neuroimage* **99**, 509–524 (2014).
48. C. Fisher, W. A. Freiwald, Contrasting specializations for facial motion within the macaque face-processing system. *Curr. Biol.* **25**, 261–266 (2015).
49. H. Zhang, S. Japee, A. Stacy, M. Flessert, L. G. Ungerleider, Anterior superior temporal sulcus is specialized for non-rigid facial motion in both monkeys and humans. *Neuroimage* **218**, 116878 (2020).
50. P. E. Downing, Y. Jiang, M. Shuman, N. Kanwisher, A cortical area selective for visual processing of the human body. *Science* **293**, 2470–2473 (2001).
51. M. V. Peelen, A. P. Atkinson, F. Andersson, P. Vuilleumier, Emotional modulation of body-selective visual areas. *Soc. Cogn. Affect. Neurosci.* **2**, 274–283 (2007).
52. I. D. Popivanov, J. Jastorff, W. Vanduffel, R. Vogels, Stimulus representations in body-selective regions of the macaque cortex assessed with event-related fMRI. *Neuroimage* **63**, 723–741 (2012).
53. K. S. Weiner, K. Grill-Spector, Neural representations of faces and limbs neighbor in human high-level visual cortex: evidence for a new organization principle. *Psychol. Res.* **77**, 74–97 (2013).
54. R. T. Born, D. C. Bradley, Structure and function of visual area MT. *Annu. Rev. Neurosci.* **28**, 157–189 (2005).
55. E. A. DeYoe, D. C. Van Essen, Concurrent processing streams in monkey visual cortex. *Trends Neurosci.* **11**, 219–226 (1988).
56. L. L. Lui, M. G. P. Rosa, Structure and function of the middle temporal visual area (MT) in the marmoset: Comparisons with the macaque monkey. *Neurosci. Res.* **93**, 62–71 (2015).
57. H. Saito *et al*., Integration of direction signals of image motion in the superior temporal sulcus of the macaque monkey. *J. Neurosci.* **6**, 145–157 (1986).
58. L. G. Ungerleider, R. Desimone, Cortical connections of visual area MT in the macaque. *J. Comp. Neurol.* **248**, 190–222 (1986).
59. H. Abe *et al*., Axonal projections from the middle temporal area in the common marmoset. *Front. Neuroanat.* **12**, 89 (2018).
60. J. L. Ji *et al*., Mapping the human brain's cortical-subcortical functional network organization. *Neuroimage* **185**, 35–57 (2019).
61. B. T. Yeo *et al*., The organization of the human cerebral cortex estimated by intrinsic functional connectivity. *J. Neurophysiol.* **106**, 1125–1165 (2011).
62. M. D. Fox *et al*., The human brain is intrinsically organized into dynamic, anticorrelated functional networks. *Proc. Natl. Acad. Sci. U.S.A.* **102**, 9673–9678 (2005).
63. A. M. Belcher *et al*., Large-scale brain networks in the awake, truly resting marmoset monkey. *J. Neurosci.* **33**, 16796–16804 (2013).
64. C. Liu *et al*., Anatomical and functional investigation of the marmoset default mode network. *Nat. Commun.* **10**, 1975 (2019).
65. M. Ghahremani, R. M. Hutchison, R. S. Menon, S. Everling, Frontoparietal functional connectivity in the common marmoset. *Cereb. Cortex* **27**, 3890–3905 (2017).
66. L. Ma *et al*., Single-unit activity in marmoset posterior parietal cortex in a gap saccade task. *J. Neurophysiol.* **123**, 896–911 (2020).
67. I. Sani *et al*., The human endogenous attentional control network includes a ventrotemporal cortical node. *Nat. Commun.* **12**, 360 (2021).
68. P. Majka *et al*., Histology-based average template of the marmoset cortex with probabilistic localization of cytoarchitectural areas. *Neuroimage* **226**, 117625 (2021).
69. J. Sliwa, W. A. Freiwald, A dedicated network for social interaction processing in the primate brain. *Science* **356**, 745–749 (2017).
70. R. B. Mars *et al*., On the relationship between the "default mode network" and the "social brain". *Front. Hum. Neurosci.* **6**, 189 (2012).
71. L. Schilbach, S. B. Eickhoff, A. Rotarska-Jagiela, G. R. Fink, K. Vogeley, Minds at rest? Social cognition as the default mode of cognizing and its putative relationship to the "default system" of the brain. *Conscious. Cogn.* **17**, 457–467 (2008).
72. K. D. Johnston, K. Barker, L. Schaeffer, D. Schaeffer, S. Everling, Methods for chair restraint and training of the common marmoset on oculomotor tasks. *J. Neurophysiol.* **119**, 1636–1646 (2018).
73. K. Gilbert *et al*., "An paralleltransmit, parallel-receive coil for routine scanning on a 7T head-only scanner" in *Proceedings of the 23rd Annual Meeting of ISMRM* (Toronto, Canada, 2015).
74. W. B. Handler *et al*., Design and construction of a gradient coil for high resolution marmoset imaging. *Biomed. Phys. Eng. Express* **6**, 045022 (2020).
75. Y. Hori, everlingmarmoset: moviedriven-fMRI. https://github.com/everlingmarmoset/moviedriven-fMRI. Deposited 25 August 2021.